PERGAMON

International Journal of Heat and Mass Transfer 45 (2002) 4409–4415

International Journal of
HEAT and MASS TRANSFER

www.elsevier.com/locate/ijhmt

Pool boiling heat transfer in binary mixtures of ammonia/water

Toshiaki Inoue [a,*], Masanori Monde [b], Yoshio Teruya [c]

[a] *Department of Mechanical Engineering, Kurume Institute of Technology, 2228 Kamitsu, Kurume, Fukuoka 830-0052, Japan*
[b] *Department of Mechanical Engineering, Saga University, 1 Honjo, Saga, 840-8502, Japan*
[c] *Laboratory of Chemistry, Kurume Institute of Technology, 2228 Kamitsu, Kurume, Fukuoka 830-0052, Japan*

Received 12 April 2001; received in revised form 15 April 2002

Abstract

Nucleate boiling heat transfer coefficients were measured during pool boiling of the mixtures of ammonia/water on a horizontal heated wire. The experiment was carried out at pressures of 0.4 and 0.7 MPa, at heat fluxes below 2000 kW/m^2 and over all ranges of fraction. The heat transfer coefficients in the mixtures are markedly less than those in single component substances and, in particular, are dramatically deteriorated in the vicinity of both single component substances. An applicability of existing correlations to the present experimental data is discussed. As a result, it is difficult for any existing correlation to predict the coefficients over all ranges of fraction.

In the mixtures of ammonia/water, heat of dilution and of dissolution are generated near a vapor–liquid interface, while vapor with a richer concentration of ammonia is condensed and then diffused into a bulk liquid; while in most other mixtures, little heat is generated during any dilution and dissolution. The effect of the heat of dilution and of dissolution on pressure and temperature in a system (pressure vessel) is shown.

1. Introduction

In mixtures of ammonia/water, each component has a larger difference in saturation temperatures and the difference between dew and boiling point is also large in comparison with other mixtures, as shown in Fig. 1. Phase equilibrium data in Fig. 1 were calculated using modified the BWR method [1] for Freon mixtures and using the Ibrahim and Klein [2] equation in PROPATH [3] for ammonia/water. Therefore, in a heat cycle whose temperatures of heat source and sink vary domestically, one can improve irreversibility of a heat exchanger by using present mixtures as a working fluid. However, there is only one paper [4] that measured the heat transfer coefficient of ammonia/water in pool boiling. In the paper, the heat of dilution and of dissolution generated near the vapor–liquid interface was not discussed.

In the present study, boiling heat transfer coefficients of ammonia/water were measured on a horizontal heated wire at pressures of 0.4 and 0.7 MPa, at heat fluxes below 2000 kW/m^2 and over all ranges of mass fraction. The applicability of five existing correlations proposed by Stephan and Körner [5], Jungnickel et al. [6], Schlünder [7], Inoue et al. [8] and Fujita and Tsutsui [9] to the measured data will be discussed.

It is already well known that the heat is generated while ammonia is mixed into water. In the present mixtures also, the heat of mixing (dilution and dissolution) is generated while vapor with a richer fraction of ammonia than the fraction of the bulk liquid is condensed and mixed into the bulk liquid. The effect of the heat of mixing on the pressure and the temperature in a system (pressure vessel) will be also clarified.

2. Experimental apparatus and procedure

Fig. 2 shows a schematic diagram of an experimental apparatus. A platinum wire 2 (diameter 0.3 mm, length 37 mm) employed as a heated wire is horizontally

---

[*] Corresponding author. Tel.: +81-942-22-2345; fax: +81-942-22-7119.

E-mail address: inoue@cc.kurume-it.ac.jp (T. Inoue).

0017-9310/02/$ - see front matter © 2002 Elsevier Science Ltd. All rights reserved.
PII: S0017-9310(02)00153-9

Nomenclature

A_0	empirical parameter in Eq.(1)
B_0	empirical parameter in Eq.(3)
C	mass fraction of ammonia
D	mass diffusivity
h	heat transfer coefficient
H_{fg}	latent heat of vaporization
h_{id}	ideal heat transfer coefficient $= 1/\{(x_1/h_1) + (x_2/h_2)\}$ in Eqs. (1) and (3)–(5) $= x_1h_1 + x_2h_2$ in Eq. (2)
k_0	parameter in Eq. (2)
k	empirical parameter in Eqs. (4) and (5)
P	pressure
Q	heat generated
q	heat flux
T	temperature
T_1, T_2, T_3	local temperature in Figs. 2 and 5
ΔT_E	temperature difference between dew and boiling point
ΔT_{id}	ideal wall superheat $= x_1\Delta T_{sat,1} + x_2\Delta T_{sat,2}$
ΔT_{sat}	wall superheat
x, y	molar fractions of liquid and vapor, respectively
ρ_ℓ, ρ_v	densities of liquid and vapor, respectively

Subscripts

1	more volatile component
2	less volatile component
c	condensed surface
i	vapor–liquid interface
id	ideal
l	liquid
s	saturation
sol	solution
v	vapor
w	wall

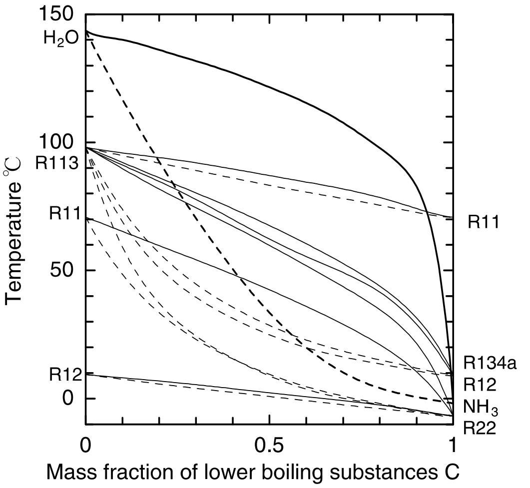

Fig. 1. Phase equilibrium diagram of mixtures at $P = 0.4$ MPa: (—) dew point curve; (- - -) boiling point curve.

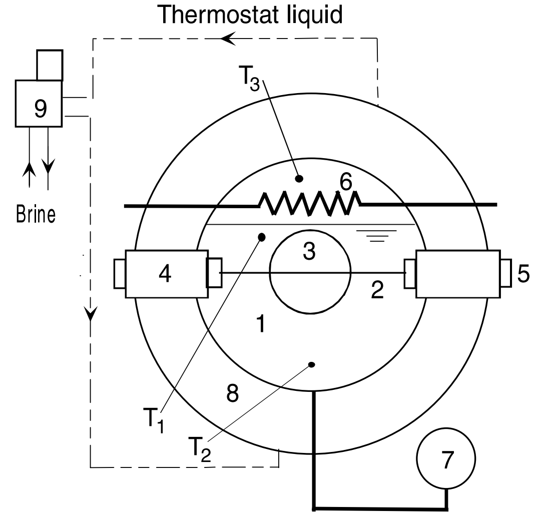

Fig. 2. Experimental apparatus: (1) Pressure vessel (2) Heated wire (3) View window (4) Insulator (5) Electrode (6) Condenser (7) Pressure gauge (8) Thermostat bath (9) Thermostat with pump T_1, T_2, T_3 thermocouples.

blanketed in location of 20 mm under a vapor–liquid interface in a pressure vessel 1 and is heated through direct electric current. Wall superheat is measured using the temperature–electric resistance characteristic of the platinum wire, which is determined by prior experiment. The pressure vessel is immersed in a thermostat bath 8 to isolate it from the surroundings. Vapor generated is condensed by a condenser 6 and is returned into bulk liquid.

Heat flux to the heated wire is increased stepwise and wall superheat, heat flux and temperature (T_1, T_2 and T_3) are measured at each heat flux after the mean temperature of the wire became steady at a given heat flux. The temperature T_1 is measured at a place of 10 mm under vapor–liquid interface and T_2 and T_3 are done near the wall of the pressure vessel. The system pressure is kept constant by controlling the supply of cooling liquid to the condenser during the experiment. Additional details of the experimental apparatus and procedure, as well as an accuracy of measurement, are not explained here since those were already indicated in Ref. [10].

3. Preliminary discussion of the effect of heat of dilution and of dissolution on the pressure and temperature in the system

Fig. 3 shows the change in the pressure and the bulk liquid temperature, T_1 and T_2, with increasing heat flux, while keeping the saturation vapor temperature, T_3, constant at mass fraction of $C = 0.5$ and 1.0. The system pressure and the bulk liquid temperature are constant with increasing heat flux for $C = 1.0$ (ammonia), while the pressure and the temperature are increased with increasing heat flux for $C = 0.5$. It is plain enough to see that heat is generated near the liquid surface because the liquid temperature, T_1, near the vapor–liquid interface increases. The heat of dilution and of dissolution causes this phenomenon. The former is generated while condensed liquid that has a richer ammonia fraction than the fraction of the bulk liquid mixes into the bulk liquid, and the latter results while ammonia vapor dissolves into the bulk liquid. Therefore, the heat generated must be smoothly removed to keep the system pressure constant during boiling.

Fig. 4 shows the change in the vapor temperature, T_3, with increasing heat flux at 0.4 MPa. The change is small at $C = 0.1$ and 1, while T_3 must be decreased after the onset of boiling in order to keep the system pressure constant at $C = 0.3$ and 0.5. This fact means that the temperature, T_3, near the condenser must be kept below saturation temperature to cool in the vapor region the heat generated at the liquid surface. Thus attention must be paid to a unique phenomenon in which the heat of mixing is greatly generated in ammonia/water, differing from mixtures without the heat of mixing.

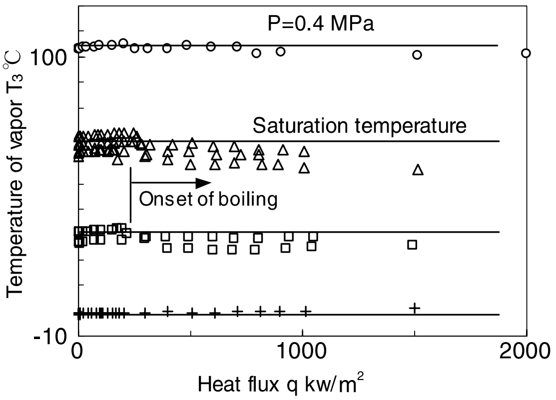

Fig. 4. Change of vapor temperature with heat flux, (○)$C = 0.1$; (△)$C = 0.3$; (□)$C = 0.5$; (+)$C = 1.0$.

Fig. 5 shows the heat generated and heat transmission in the system estimated from the pressure and the temperature in Fig. 3. The heat is transmitted from the vapor–liquid interface toward the circumference as shown in Fig. 5. However, convection heat transfer coefficients, h_v, are small since convection of vapor is very gentle in the vessel, and the thermal conductivity of vapor is also very small. Therefore, the temperature difference, $T_i - T_c$, between the vapor–liquid interface and the condenser must be large in order to keep the pressure constant. The temperature difference, $T_1 - T_3$, is also increased with increasing heat flux as shown in Fig. 3,

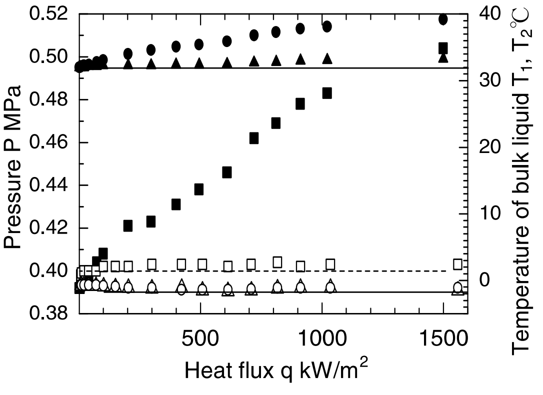

Fig. 3. Change in pressure and bulk liquid temperature with heat flux at 0.4 MPa. (—) Saturation temperature; (- - -) saturation pressure. $C = 0.5$, $T_3 = 32$ °C, ■ pressure; ● temperature T_1, ▲ temperature T_2. $C = 1.0$, $T_3 = -1.9$ °C, □ pressure; ○ temperature T_1, △ temperature T_2.

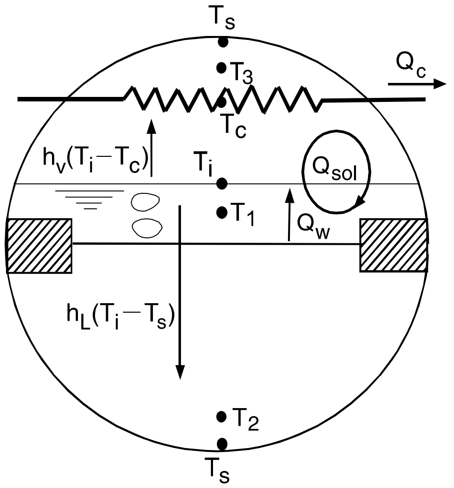

Fig. 5. Heat generated in the system.

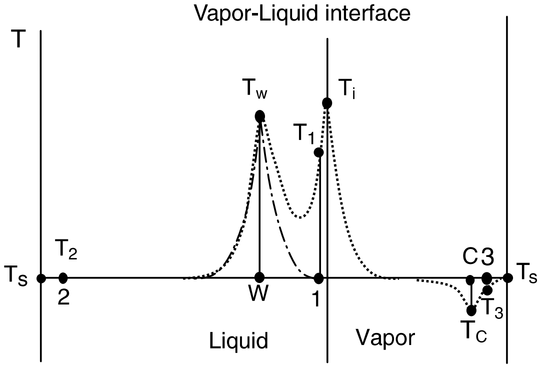

Fig. 6. Temperature distribution in the system, (1, 2, 3): position of thermocouples; (C): position of condenser; (W): position of heated wire.

since the amount of vapor generated increases with increasing heat flux. Well, it will become easy to control the condenser, since $T_1 - T_3$ becomes small if h_v is large.

Fig. 6 shows a temperature distribution in the vessel estimated from Figs. 3 and 4, during a steady boiling in a heat flux. The temperature distribution is tentatively drawn with a broken line, since the exact distribution is unknown. A temperature distribution for no heat generated during mixing is shown with a dot-dash line for reference. The temperature is highest at the vapor–liquid interface or on the heated wire; becomes lower than the saturation temperature near the condenser; and gradually increases to the saturation temperature of circumference, in the vapor space. Heat is accumulated near some point of the lowest temperature between the heated wire and the interface, some of which seems to be consumed by growth of vapor bubbles and the remainder of which may be diffused into the surrounding liquid well. The boiling heat transfer coefficients were measured under a steady state with temperature distribution as shown in Fig. 6. Therefore, it should be noted that special attention is needed to control the condenser in order to keep the system pressure constant. It is estimated that the heat generated gives little influence on the heat transfer coefficients because the pressure is kept constant and the influence of the heat of mixing does not reach the heated wire. This is due to the phenomenon of heat generation near the vapor–liquid interface. Here, the heat transfer coefficient is defined by $h = q/(T_W - T_S)$.

4. Experimental result

4.1. Boiling heat transfer in single component substances

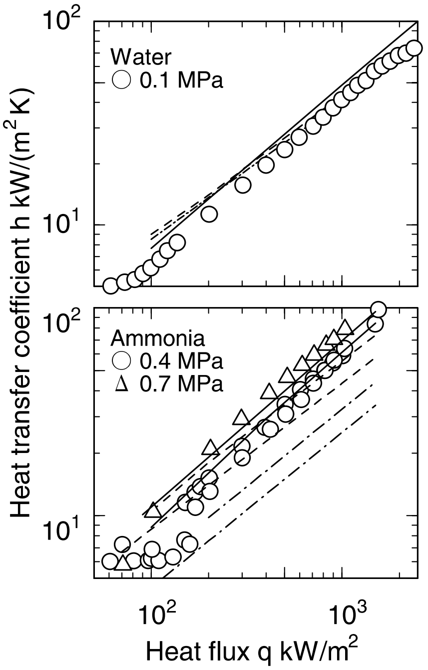

Fig. 7. Comparison between present data and correlations in pure substances. Correlations: (—) Nishikawa and Fujita [10]; (– – –) Kutateladze [11]; (– · – · –) Stephan and Abdelsalam [12].

Fig. 7 shows a comparison between heat transfer data obtained by the present experiment and correlations proposed by Nishikawa and Fujita [11] (equation for high heat flux with $f_\zeta = 0.39$), Kutateladze [12] and Stephan and Abdelsalam [13]. Their correlations can predict the data for water at 0.1 MPa within an accuracy of 15%. For ammonia, the correlations [11,12] are in good agreement with the data, though reference [13] under-predicts the data. Therefore the Nishikawa and Fujita [11] correlation, which is a figure necessary for predicting the boiling heat transfer coefficients of ammonia/water mixtures, is employed to predict boiling heat transfer coefficients in water and ammonia at 0.4 and 0.7 MPa.

4.2. Boiling heat transfer in mixtures of ammonia/water

Fig. 8 shows the effect of the mass fraction on the heat transfer coefficients, the temperature difference between boiling and dew points, ΔT_E, and the molecular fraction difference between vapor and liquid, $y_1 - x_1$. The coefficients in the mixtures become dramatically smaller than those in both single components, and in particular are steeply decreased in the vicinity of the single component substances. The minimum values exist in wide range from $C = 0.3$ to 0.7 and would become independent of the fraction in this range. It is found that the trend in h against C is different from that in both ΔT_E and $y_1 - x_1$.

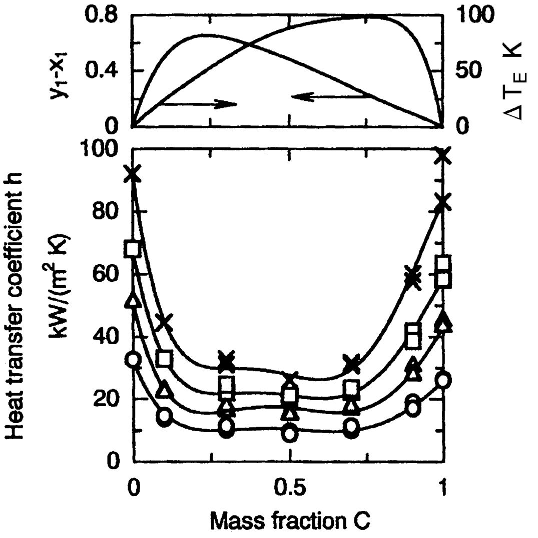

Fig. 8. Effect of mass fraction on heat transfer coefficient.

5. Discussion of correlations

Most of the existing correlations include physical properties of mixtures and empirical parameters. It is difficult to discuss the applicability of correlations, since some of them for mixtures of ammonia/water are unknown. In this study, correlations (1)–(5) were selected as listed in Table 1. These correlations use phase equilibrium data (for example, ΔT_E and $y_1 - x_1$) and some predictable quantities of state (for example, H_{fg}, ρ). Here, A_0 in Eq. (1) depends on the combination of binary mixtures and Stephan and Körner [5] found $0.42 \leqslant A_0 \leqslant 3.56$ for 17 kinds of binary mixtures. They recommended the mean value of $A_0 = 1.53$ for mixtures that are not listed in their table [5]. The constant k_0 in Eq. (2) was given as a function of the difference in saturation temperature, $|T_{S2} - T_{S1}|$, of both single component substances. The value of $k_0 = 2$ which is a maximum value was employed in this discussion, since the difference (for example, 145.5 K at 0.4 MPa) for ammonia/water is remarkably beyond the applicable range of $0 \leqslant |T_{S2} - T_{S2}| \leqslant 80$ K whose value was described by Jungnickel et al. [6]. The values of D and B_0 in Eq. (3) were recommended by Schlünder [7]. Thermodynamic properties were predicted using the Ibrahim and Klein [2] equation in PROPATH [3].

Fig. 9 shows the h–q relation at 0.4 MPa for given mass fractions. Plots and lines in Fig. 9 are the experimental data and values predicted by Eqs. (1)–(4), respectively. The data with a small inclination along the heat flux are the natural convection region. Eq. (1) over-predicts the present experimental data over all ranges of the fraction, and Eqs. (2)–(4) under-predict the data over all ranges of the fraction. Eq. (4) is almost identical with Eq. (5), though they were separately proposed.

Fig. 10 shows the comparison of the correlations with the present data. Both the Inoue et al. [8] and the Schlünder [7] equations under-predict the data at 0.4 MPa with an accuracy of −15% to −76% and −15% to −64%, respectively. The trend in under-predicting reverses, depending on the mass fraction. The Jungnickel et al. [6] equation begins to under-predict the data with increasing heat flux from Fig. 9. The Stephan and Körner [5] equation using $A_0 = 1.53$ over-predicts the data over all ranges of fraction (+4% to +78%) and, especially, extremely over-predicts the data at $C = 0.5$ and 0.7, which has the same characteristic as Schlünder's. It should be added that it is difficult to accurately discuss the data at 0.7 MPa because there are scatterings in the data at that pressure. The authors modified the empirical parameter k in the Inoue et al. [8] equation (4) to meet their Eq. (4) with the data using the least mean square method. Nevertheless, there was still a large predictive error of ±48%.

Table 1
Existing correlations

Stephan and Körner [5]	$\frac{h}{h_{id}} = \frac{1}{1 + A_0(0.88 + 0.12[\mathrm{bar}])(y_1 - x_1)}, \quad A_0 = 1.53$	(1)
Jungnickel et al. [6]	$\frac{h}{h_{id}} = \frac{1}{1 + k_0(y_1 - x_1)(\rho_v/\rho_\ell)q^{(0.48+0.1x_1)}}, \quad k_0 = 2$	(2)
Schlünder [7]	$\frac{h}{h_{id}} = \frac{1}{1 + (y_1 - x_1)\{1 - \exp(-B_0 q/D\rho_\ell H_{fg})\}(T_{s2} - T_{s1})\Delta T_{id}}, \quad B_0 = 1, \ D = 0.0002\ \mathrm{m/s}$	(3)
Inoue et al. [8]	$\frac{h}{h_{id}} = \frac{1}{1 + k\Delta T_E/\Delta T_{id}}, \quad k = 1 - 0.75\exp(-0.75 \times 10^{-5} q\ [\mathrm{W/m^2}])$	(4)
Fujita and Tsutsui [9]	$\frac{h}{h_{id}} = \frac{1}{1 + k\Delta T_E/\Delta T_{id}}, \quad k = 1 - 0.8\exp(-10^{-5} q\ [\mathrm{W/m^2}])$	(5)

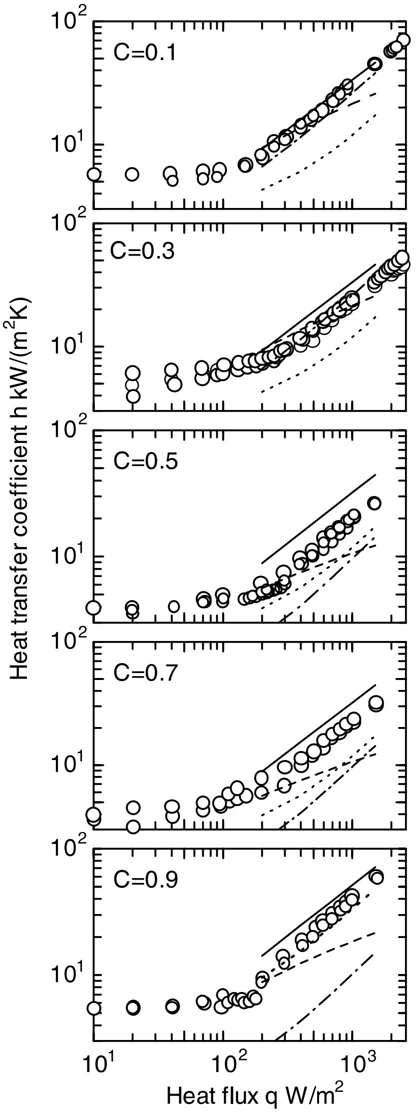

Fig. 9. Comparison of correlations with experimental data in h–C relation in mixtures. (—) Stephan and Körner [5]; (– – –) Jungnickel [6]; (- - -) Schlünder [7]; (– · – · –) Inoue et al. [8].

Consequently, any existing correlation fails to predict the present heat transfer data of ammonia/water mixtures. This failure may be attributed to the fact that Eqs. (1)–(5) are closely correlated with ΔT_E and $y_1 - x_1$, though the data are not related to both ΔT_E and $y_1 - x_1$ as shown in Fig. 8, and to the fact that ΔT_E and $y_1 - x_1$ of ammonia/water mixtures are much lager than those of mixtures that have been studied. Thus, what correlation equation taking into consideration the effect of both ΔT_E and $y_1 - x_1$ is open for discuss.

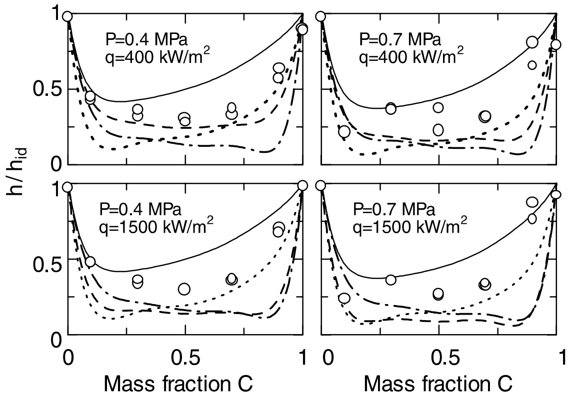

Fig. 10. Comparison of correlations with present data (curves predicted are the same with those used in Fig. 9).

6. Conclusions

The experimental study were conducted for heat transfer during nucleate pool boiling on the horizontal heated wire in the non-azeotropic binary mixtures of ammonia/water, in which the heat of mixing is generated at the vapor–liquid interface during boiling. The results are as follows:

1. The effect of the heat of dilution and of dissolution on the pressure and the temperature in the system were clarified.
2. Boiling heat transfer in ammonia can be predicted by existing correlations [11,12].
3. The heat transfer coefficients in ammonia/water mixtures become dramatically smaller than those in both single component substances and, in particular, deteriorate steeply in the vicinity of both single component substances.
4. It is difficult to predict the heat transfer coefficients in ammonia/water over all ranges of fraction using existing correlations.

Acknowledgements

The authors gratefully acknowledge Professor emeritus K. Nishikawa of Kyushu University for his valuable suggestions and encouragement for this work.

References

[1] H. Nishiumi, S. Saito, An improved generalized BWR equation of state applicable to reduce temperatures, J. Chem. Eng. Japan (8-5) (1975) 356–360.

[2] O.M. Ibrahim, S.A. Klein, Thermodynamic properties of ammonia–water mixtures, ASHRAE Transactions, Symposia, CH-93-21-2 (1993) 1495–1502.

[3] PROPATH GROUP, A Program Package for Thermo Physical Properties of Fluids, Version 11.1 (1999).

[4] V.N. Filatkin, Boiling heat transfer to water–ammonia mixtures, in: S.S. Ktateladze (Ed.), Problems of Heat Transfer and Hydraulics of Two Phase Media, Pergamon Press, 1969 (in Russian).

[5] K. Stephan, M. Körner, Berechnung des Wärme-übergangs Verdampfender Binärer Flüssigkeitgemische, Chmie-Ing Techn. 41 (1969) 409–417.

[6] H. Jungnickel, P. Wassilew, W.E. Kraus, Investigations on the heat transfer of binary refrigerant mixtures, Int. J. Refrig. 3 (1980) 129–133.

[7] E.U. Schlünder, Heat transfer in nucleate boiling of mixtures, Int. Chem. Eng. 23 (1983) 589–599.

[8] T. Inoue, N. Kawae, M. Monde, Characteristics of heat transfer coefficient during nucleate pool boiling of binary mixtures, Heat Mass Transfer 33 (1998) 337–344.

[9] Y. Fujita, M. Tsutsui, Heat transfer in nucleate pool boiling of binary mixtures, Int. J. Heat Mass Transfer 37 (1994) 291–302.

[10] T. Inoue, M. Monde, Nucleate pool boiling heat transfer in binary mixtures, Heat Mass Transfer 29 (1994) 171–180.

[11] K. Nishikawa, Y. Fujita, On the pressure factor in nucleate boiling heat transfer, Memoirs of the Faculty of Engineering, Kyushu University, Vol. 36 (1977) 303–341.

[12] S.S. Kutateladze, Heat Transfer in Condensation and Boiling, 2nd Ed. AEC-tr-3770 (1952).

[13] K. Stephan, M. Abdelsalam, Heat transfer correlations for natural convection boiling, Int. J. Heat Mass Transfer 5 (1980) 73–87.